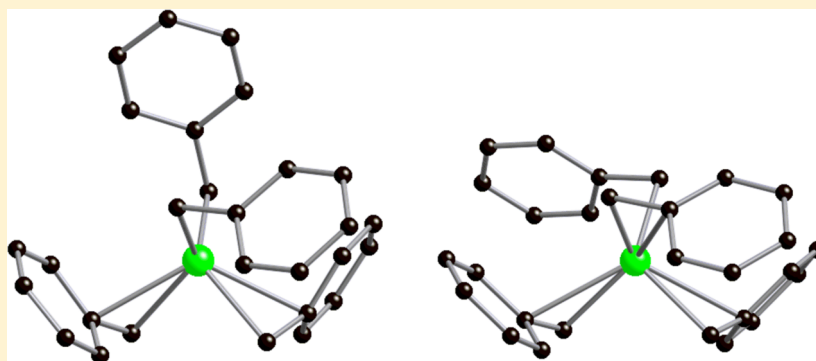


Highly Variable Zr–CH₂–Ph Bond Angles in Tetrabenzylzirconium: Analysis of Benzyl Ligand Coordination Modes

Yi Rong, Ahmed Al-Harbi, and Gerard Parkin*

Department of Chemistry, Columbia University, New York, New York 10027, United States

S Supporting Information



ABSTRACT: Analysis of a monoclinic modification of Zr(CH₂Ph)₄ by single-crystal X-ray diffraction reveals that the bond angles Zr–CH₂–Ph in this compound span a range of 25.1°, which is much larger than previously observed for the orthorhombic form (12.1°). In accord with this large range, density functional theory calculations demonstrate that little energy is required to perturb the Zr–CH₂–Ph bond angles in this compound. Furthermore, density functional theory calculations on Me₃ZrCH₂Ph indicate that bending of the Zr–CH₂–Ph moiety in the monobenzyl compound is also facile, thereby demonstrating that a benzyl ligand attached to zirconium is intrinsically flexible, such that its bending does not require a buffering effect involving another benzyl ligand.

INTRODUCTION

Benzyl ligands coordinate to transition metal centers in manifold ways. Thus, in addition to η^1 -coordination, interaction via the phenyl group is also possible, with η^2 -, η^3 -, η^4 -, η^5 -, and η^7 -coordination modes having been discussed in the literature (Figure 1).^{1,2} The coordination mode of a benzyl ligand is not

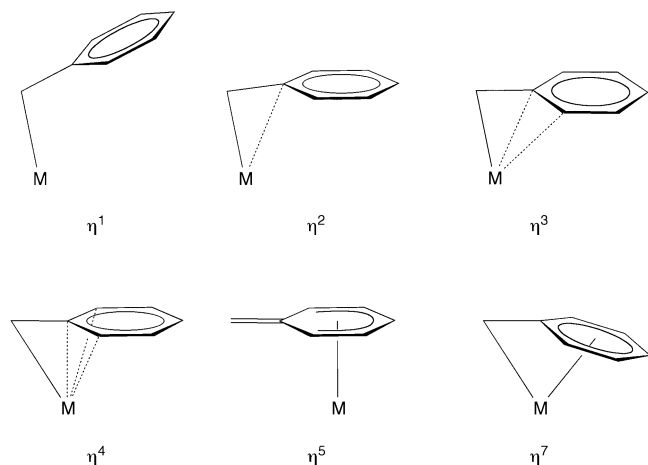


Figure 1. Benzyl ligand coordination modes discussed in the literature.

only expected to influence the intrinsic reactivity of the bond M–CH₂Ph but could also provide a means to modulate the reactivity of a metal center by stabilizing coordinatively unsaturated centers. Tetrabenzylzirconium, first reported in 1969,³ has proven to be of much value in the development of zirconium chemistry (especially with respect to the synthesis of catalysts for olefin polymerization)^{4–7} and represents an interesting example of a complex that features different benzyl coordination modes.⁸ For example, the Zr–CH₂–Ph bond angles of Zr(CH₂Ph)₄ have been reported to range from 87.0(3)° to 99.1(3)°. ^{8a} Here, we report the structure of another crystalline form of Zr(CH₂Ph)₄ that exhibits an even greater range of Zr–CH₂–Ph bond angles, namely, from 81.6(1)° to 106.7(2)°. Consistent with this large range, density functional theory calculations demonstrate that little energy is required to perturb the Zr–CH₂–Ph bond angles in this compound. In addition, we also analyze the distribution of the various benzyl coordination modes by employing the Cambridge Structural Database.⁹

Received: August 24, 2012

Table 1. Crystallographic Data for Polymorphs of $\text{Zr}(\text{CH}_2\text{Ph})_4$

	ref 8a	refs 8b,c	this work
crystallization method	<i>n</i> -heptane at -25°C	toluene at -25°C	toluene at room temp
lattice	orthorhombic	orthorhombic	monoclinic
space group	<i>Pbca</i>	<i>Pbca</i>	<i>P2</i> ₁
<i>a</i> /Å	16.387(1)	19.945(6)	10.2238(10)
<i>b</i> /Å	20.022(1)	13.716(7)	9.6635(9)
<i>c</i> /Å	13.758(6)	16.306(5)	11.2356(11)
α /deg	90	90	90
β /deg	90	90	101.295(1)
γ /deg	90	90	90
<i>V</i> /Å ³	4514(2)	4461	1088.6(2)
<i>d</i> /g cm ^{−3}	1.341	1.36	1.390
temp/K	293(2)	233	150(2)

Table 2. Metrical Data for Polymorphs of $\text{Zr}(\text{CH}_2\text{Ph})_4$

	Zr–CH ₂ –Ph/deg	Zr–CH ₂ /Å	Zr⋯C _{ipso} /Å	Zr⋯C _{ortho(short)} /Å	Zr⋯C _{ortho(long)} /Å	δ_{ipso} /Å	$\delta_{\text{ortho(short)}}$ /Å	$\delta_{\text{ortho(long)}}$ /Å
Monoclinic ^a								
C11	81.63(14)	2.270(2)	2.509(2)	3.022(2)	3.089(2)	0.24	0.75	0.82
C21	82.36(13)	2.278(2)	2.533(2)	2.969(3)	3.174(2)	0.26	0.69	0.90
C31	98.67(15)	2.262(3)	2.873(2)	3.472(2)	3.628(2)	0.61	1.21	1.37
C41	106.73(15)	2.2929(19)	3.063(2)	3.774(2)	3.820(2)	0.77	1.48	1.53
Orthorhombic ^b								
C1	87.0(3)	2.259(5)	2.614(4)	3.072(5)	3.347(6)	0.36	0.81	1.09
C2	90.2(3)	2.248(5)	2.684(4)	3.249(4)	3.361(5)	0.44	1.00	1.11
C3	93.9(3)	2.255(5)	2.773(3)	3.298(5)	3.535(4)	0.52	1.04	1.28
C4	99.1(3)	2.258(4)	2.879(4)	3.519(5)	3.589(6)	0.62	1.26	1.33

^aThis work. ^bReference 8a.

RESULTS AND DISCUSSION

Structural Characterization of Monoclinic $\text{Zr}(\text{CH}_2\text{Ph})_4$

Previous X-ray diffraction studies have revealed $\text{Zr}(\text{CH}_2\text{Ph})_4$ to exist as orthorhombic crystals, with space group *Pbca*, as summarized in Table 1. It is, therefore, noteworthy that we have obtained a monoclinic crystalline form of $\text{Zr}(\text{CH}_2\text{Ph})_4$ as illustrated in Figure 2, that differs from the previously reported

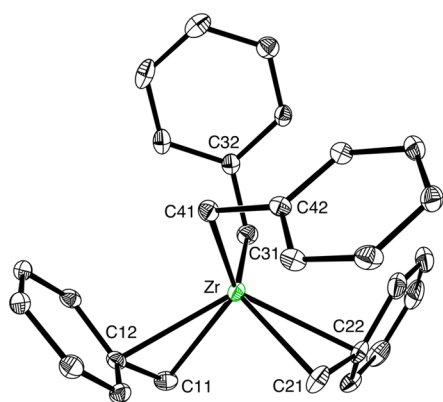


Figure 2. Molecular structure of monoclinic $\text{Zr}(\text{CH}_2\text{Ph})_4$. Hydrogen atoms are omitted for clarity.

orthorhombic structure in some significant ways. Firstly, whereas the conformation of the benzyl ligands in orthorhombic $\text{Zr}(\text{CH}_2\text{Ph})_4$ are arranged in such a manner as to give an approximate *S*₄ molecular symmetry, the molecular structure of the monoclinic form deviates considerably from this idealized geometry, as illustrated in Figure 3. The two most notable features that remove the *S*₄ symmetry for the

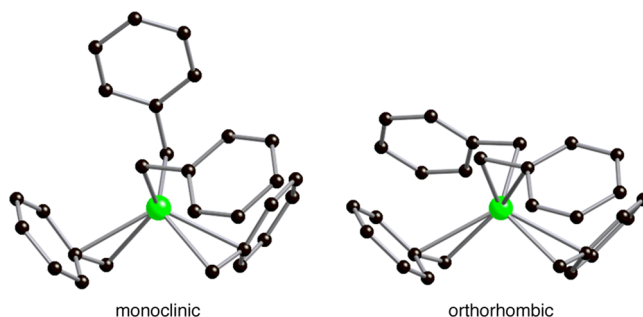


Figure 3. Comparison of the molecular structure of monoclinic (left) and orthorhombic (right) forms of $\text{Zr}(\text{CH}_2\text{Ph})_4$. Hydrogen atoms are omitted for clarity.

monoclinic structure are (i) the dihedral angle between the two [C–Zr–C] planes¹⁰ is reduced from 90° to 69° and (ii) one of the benzyl ligands points in a direction that destroys the *C*₂ axis. Secondly, in addition to this variation in conformation, the zirconium–benzyl interactions in the two polymorphs are also different (Table 2). For example, the Zr–CH₂–Ph bond angles of the monoclinic form span a range of 25.1° , which is substantially greater than for the orthorhombic form (12.1°). Furthermore, monoclinic $\text{Zr}(\text{CH}_2\text{Ph})_4$ exhibits Zr–CH₂–Ph angles that are both more acute (81.6°) and more obtuse (106.7°) than observed for the orthorhombic form, for which the range is 87.0 – 99.1° .

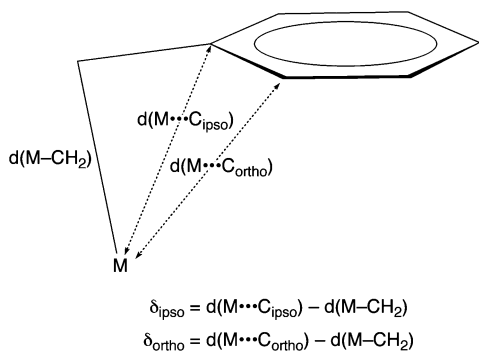
Classification of Benzyl Ligands in $\text{Zr}(\text{CH}_2\text{Ph})_4$: Criteria for Identifying the Benzyl Ligand Coordination Mode. While the M–CH₂–Ph bond angle distinguishes whether a benzyl ligand coordinates in an η^1 -manner (with an idealized value of 109.5°) or an η^π -manner ($x > 1$), differentiation

Table 3. Metrical Data for Selected Benzyl Ligand Coordination Modes

	M–CH ₂ –Ph/deg	$\delta_{\text{ipso}}/\text{\AA}$	$\delta_{\text{ortho(short)}}$ /\AA	$\delta_{\text{ortho(long)}}$ /\AA	$\delta_{\text{meta(short)}}$ /\AA	$\delta_{\text{meta(long)}}$ /\AA	$\delta_{\text{para}}/\text{\AA}$	notes
η^1	109.5	0.84	0.85–1.58	1.58–2.21	2.20–2.75	2.75–3.23	3.24	a
η^2	90.0	0.44	1.10	1.10	2.14	2.14	2.57	b
η^2	97.0	0.59	1.27	1.27	2.36	2.36	2.81	c
η^3	69.3	0	0	1.14	1.14	1.96	1.96	d
η^4	57.4	–0.42	0	0	0.69	0.69	0.98	e
η^7	62.1	–0.30	–0.12	–0.10	–0.03	–0.02	–0.10	f

^aDerived values for an idealized M–CH₂–Ph = 109.5° obtained by using the CSD averages $d(\text{M–CH}_2\text{Ph}) = 2.195 \text{ \AA}$ and $d(\text{CH}_2\text{–C}_{\text{ipso}}) = 1.483 \text{ \AA}$ for η^1 -benzyl compounds. The ranges for δ_{ortho} and δ_{meta} correspond to rotation about the C–Ph bond. ^bDerived values for an idealized M–CH₂–Ph = 90.0° obtained by using the CSD averages $d(\text{M–CH}_2\text{Ph}) = 2.300 \text{ \AA}$ for η^2 -benzyl compounds and $d(\text{CH}_2\text{–C}_{\text{ipso}}) = 1.483 \text{ \AA}$. Values for δ_{ortho} and δ_{meta} are for a M–C–C–C torsion angle of 90°. ^cDerived values for M–CH₂–Ph = 97.0° obtained by using the CSD averages $d(\text{M–CH}_2\text{Ph}) = 2.300 \text{ \AA}$ for η^2 -benzyl compounds and $d(\text{CH}_2\text{–C}_{\text{ipso}}) = 1.483 \text{ \AA}$. Values for δ_{ortho} and δ_{meta} are for a M–C–C–C torsion angle of 90°. ^dDerived values obtained assuming that $d(\text{M–CH}_2\text{Ph}) = 2.090 \text{ \AA}$, which is the average of known η^3 -compounds, and that $d(\text{M–CH}_2\text{Ph}) = d(\text{M–C}_{\text{ortho(short)}}$). ^eDerived values obtained assuming that $d(\text{M–CH}_2\text{Ph}) = 2.653 \text{ \AA}$, corresponding to that in the only known η^7 -compound, and that $d(\text{M–CH}_2\text{Ph}) = d(\text{M–C}_{\text{ortho(short)}}$) = $d(\text{M–C}_{\text{ortho(long)}}$). ^fValues listed are for the only structurally reported η^7 -compound.

between the various expanded hapticities requires analysis of the M···C distances involving the phenyl group.^{1a,b,8a} Specifically, as the hapticity increases, the *ipso*, *ortho*, *meta*, and *para* carbon atoms approach the metal center and the coordination mode can be classified by comparing the M···C_{ipso}, M···C_{ortho}, M···C_{meta}, and M···C_{para} distances to the M–CH₂ bond length, i.e., δ_{ipso} , δ_{ortho} , δ_{meta} , and δ_{para} (Figure 4), an approach that is based on Andersen's analysis.^{1a}

Figure 4. Definition of δ_{ipso} and δ_{ortho} .

With respect to interpreting these values, it is first pertinent to consider some idealized situations (Table 3). For example, an η^1 -benzyl ligand with an idealized M–CH₂–Ph tetrahedral angle of 109.5° is characterized by a δ_{ipso} value of 0.84 Å, while an η^2 -benzyl ligand with a M–CH₂–Ph angle of 90.0° is characterized by a δ_{ipso} value of 0.44 Å. An idealized η^3 -benzyl ligand is characterized by a situation in which the M–CH₂–Ph angle is <90.0° and one of the *ortho* carbon atoms approaches the metal center within a distance that is comparable to that of the methylene carbon; that is, δ_{ipso} and $\delta_{\text{ortho(short)}}$ have values of 0.0 Å. An idealized η^4 -benzyl ligand requires both δ_{ortho} values to be 0.0 Å, while an idealized η^7 -benzyl ligand also requires all δ_{meta} and δ_{para} values to be 0.0 Å.

Despite the idealized data presented in Table 3, the classification of the coordination mode of the benzyl ligand in a compound is, nevertheless, a subjective issue. For example, a compound with a M–CH₂–Ph angle as small as 97.1° has been classified as η^1 ,¹¹ while a compound with a M–CH₂–Ph angle as large as 97.5° has been classified as η^2 .^{12,13} However, all other compounds listed in the Cambridge Structural Database⁹ that have been assigned η^2 -benzyl coordination have bond angles M–CH₂–Ph less than 97°. ¹⁴ On this basis, we propose

Table 4. Criteria for Assigning Benzyl Ligand Coordination Modes

	M–CH ₂ –Ph/deg	$\delta_{\text{ipso}}/\text{\AA}$	$\delta_{\text{ortho(short)}}$ /\AA	$\delta_{\text{ortho(long)}}$ /\AA
η^1	>97	>0.5		
η^2	≤97	≤0.5		
η^3	≤97	≤0.5	≤0.5	>0.5
η^4	≤90	<0.0	≤0.5	≤0.5

that a M–CH₂–Ph angle of ≤97° be used as a criterion for η^2 -coordination (Table 4), recognizing that such distinctions have little meaning at the borderline. With respect to distinguishing between η^2 - and η^3 -benzyl coordination, we propose that the latter is identified by $\delta_{\text{ortho(short)}} \leq 0.5 \text{ \AA}$, on the basis that Zr–arene bond lengths¹⁵ may be up to ca. 0.5 Å longer than the mean Zr–CH₂Ph bond length for compounds listed in the Cambridge Structural Database (2.298 Å).

A plot of M–CH₂–Ph bond angle versus $\delta_{\text{ortho(short)}}$ (Figure 5) illustrates the regions that correspond to η^1 -, η^2 -, and η^3 -benzyl coordination modes, and examples of compounds that belong to these classes are provided in Table 5.^{16–31} Of these coordination modes, η^1 is the most prevalent (92.9%), followed by η^2 (6.1%) and η^3 (0.9%). η^4 -Benzyl coordination requires small values for both $\delta_{\text{ortho(short)}}$ and $\delta_{\text{ortho(long)}}$, and analysis of the compounds listed in the

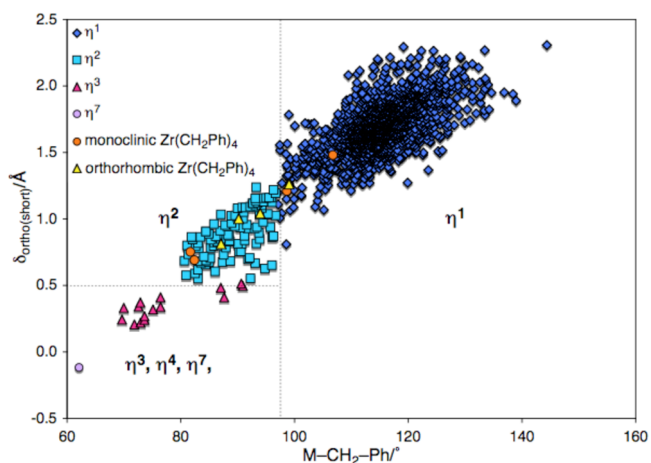


Figure 5. Classification of benzyl ligands according to M–CH₂–Ph bond angle and δ_{ortho} . η^1 -Coordination (92.9%) is the most prevalent, followed by η^2 (6.1%), η^3 (0.9%), and η^7 (0.1%).

Table 5. Examples of Benzyl Compounds Classified According to Their Coordination Mode^a

	compound	M–CH ₂ –Ph/deg	$\delta_{\text{ipso}}/\text{\AA}$	$\delta_{\text{ortho(short)}}$ /\AA	$\delta_{\text{ortho(long)}}$ /\AA	ref
η^1	$(\eta^2\text{-}3,5\text{-Me}_2\text{Pz})_2\text{Zr}(\eta^1\text{-CH}_2\text{Ph})(\eta^2\text{-CH}_2\text{Ph})$	97.1	0.59	1.11	1.39	11
	$[\text{OONO}] \text{Zr}(\eta^1\text{-CH}_2\text{Ph})_2$	98.6	0.62	1.19	1.41	13
	$[\eta^3\text{-MeC}(\text{NC}_7\text{H}_6)\text{CHC}(\text{N-}p\text{-Tol})\text{Me}] \text{Zr}(\eta^1\text{-CH}_2\text{Ph})(\eta^2\text{-CH}_2\text{Ph})$	99.6	0.64	1.31	1.35	19
	$\{[2,6\text{-CH}_2\text{N}(\text{C}_6\text{F}_5)]_2\text{NC}_5\text{H}_3\}_2\text{Zr}(\eta^1\text{-CH}_2\text{Ph})(\eta^2\text{-CH}_2\text{Ph})$	104.2	0.73	1.19	1.69	17
	$[\eta^2\text{-N}(\text{CHMePh})(\text{PPh}_3)] \text{Zr}(\eta^1\text{-CH}_2\text{Ph})_2(\eta^2\text{-CH}_2\text{Ph})$	108.3	0.80	1.26	1.78	18
	$[\text{NNO}] \text{Zr}(\eta^1\text{-CH}_2\text{Ph})(\eta^2\text{-CH}_2\text{Ph})$	106.7	0.77	1.37	1.61	14c
	$[\eta^2\text{-N}(\text{CHMePh})(\text{PPh}_3)] \text{Zr}(\eta^1\text{-CH}_2\text{Ph})_2(\eta^2\text{-CH}_2\text{Ph})$	115.8	0.94	1.67	1.74	18
	$(\text{pyCMe}_2\text{O})_2\text{Zr}(\eta^1\text{-CH}_2\text{Ph})(\eta^2\text{-CH}_2\text{Ph})$	116.6	0.95	1.61	1.81	14d
	$(\text{Cp}^{1,2,4\text{-Bu}^1_3})\text{CeCH}_2\text{Ph}$	130.4	1.12	1.82	2.03	34
	$\text{Tp}^*\text{Zr}(\eta^1\text{-CH}_2\text{Ph})_3$	144.4	1.31	2.02	2.31	16
η^2	$[\eta^2\text{-N}(\text{CHMePh})(\text{PPh}_3)] \text{Zr}(\eta^1\text{-CH}_2\text{Ph})_2(\eta^2\text{-CH}_2\text{Ph})$	82.5	0.25	0.59	0.99	18
	$\text{Cp}^*\text{Mo}(\text{NO})(\text{CH}_2\text{SiMe}_3)(\eta^2\text{-CH}_2\text{Ph})$	83.0	0.29	0.82	0.98	1d
	$[\eta^3\text{-MeC}(\text{NC}_7\text{H}_6)\text{CHC}(\text{N-}p\text{-Tol})\text{Me}] \text{Zr}(\eta^1\text{-CH}_2\text{Ph})(\eta^2\text{-CH}_2\text{Ph})$	83.6	0.28	0.67	0.98	19
	$\text{Cp}^*\text{Th}(\eta^2\text{-CH}_2\text{Ph})_3$	84.1	0.25	0.72	0.97	21
	$[\text{Cp}_2\text{Zr}(\text{CH}_3\text{CN})(\eta^2\text{-CH}_2\text{Ph})][(\text{BPh}_4)]$	84.4	0.31	0.91	0.93	20
	$\{[2,6\text{-CH}_2\text{N}(\text{C}_6\text{F}_5)]_2\text{NC}_5\text{H}_3\}_2\text{Zr}(\eta^1\text{-CH}_2\text{Ph})(\eta^2\text{-CH}_2\text{Ph})$	84.5	0.31	0.69	1.04	17
	$\text{Cp}^*\text{U}(\eta^2\text{-CH}_2\text{Ph})_3$	85.4	0.29	0.88	0.95	22
	$\text{Cp}^*\text{Th}(\eta^2\text{-CH}_2\text{Ph})_3$	85.8	0.31	0.80	0.92	21
	$\text{Cp}^*\text{U}(\eta^2\text{-CH}_2\text{Ph})_3$	87.1	0.32	0.89	0.97	22
	$\text{Cp}^*\text{U}(\eta^2\text{-CH}_2\text{Ph})_3$	87.3	0.34	0.90	0.94	22
	$\text{Cp}^*\text{Th}(\eta^2\text{-CH}_2\text{Ph})_3$	90.3	0.40	0.75	1.25	21
	$(\text{Cp}^{1,2,4\text{-Bu}^1_3})\text{CeCH}_2\text{Ph}$	93.1	0.44	0.67	1.41	34
	$[\text{NNO}] \text{Zr}(\eta^1\text{-CH}_2\text{Ph})(\eta^2\text{-CH}_2\text{Ph})$	95.8	0.55	0.94	1.47	14c
	$(\text{pyCMe}_2\text{O})_2\text{Zr}(\eta^1\text{-CH}_2\text{Ph})(\eta^2\text{-CH}_2\text{Ph})$	96.1	0.55	1.13	1.31	14d
η^3	$\text{Ni}(\text{PMe}_3)(\eta^1\text{-CH}_2\text{Ph})(\eta^3\text{-CH}_2\text{Ph})$	69.7	0.02	0.24	0.82	28
	$\text{Ni}(\text{PMe}_3)(\eta^1\text{-CH}_2\text{Ph})(\eta^3\text{-CH}_2\text{Ph})$	70.0	0.03	0.33	0.76	28
	$\{\kappa^2\text{-C}_6\text{N}(\text{Ar})\text{N}=\text{C}(\text{Me})\text{C}(\text{CH}_2)[\text{OB}(\text{C}_6\text{F}_5)_3]\}\text{Ni}(\eta^3\text{-CH}_2\text{Ph})$ (Ar = 2,6-Pr ⁱ ₂ C ₆ H ₃)	71.8	0.07	0.21	0.98	30
	$[\kappa^2\text{-P}_3\text{O}_2\text{-P}(\text{Cy})_2\text{-}4\text{-Me-C}_6\text{H}_3(\text{SO}_3)]\text{Ni}(\eta^3\text{-CH}_2\text{Ph})$	72.6	0.10	0.34	0.94	31
	$[\text{P}(\text{OCH}_3)_3]_3\text{Co}(\eta^3\text{-CH}_2\text{Ph})$	72.9	0.08	0.37	1.01	25
	$[\text{Pr}^i_3\text{P}(\text{CH}_2)_3\text{PPr}^i_2]\text{Rh}(\eta^3\text{-CH}_2\text{Ph})$	72.9	0.06	0.22	0.95	26
	$[\kappa^2\text{-P}_3\text{C-}2\text{-P}(2\text{-OMePh})_2\text{-}4\text{-Me-C}_6\text{H}_3(\text{SO}_3)]\text{Ni}(\eta^3\text{-CH}_2\text{Ph})$	73.6	0.12	0.24	1.09	31
	$[\kappa^2\text{-P}_3\text{O}_2\text{-P}(\text{Cy})_2\text{-}4\text{-Me-C}_6\text{H}_3(\text{SO}_3)]\text{Ni}(\eta^3\text{-CH}_2\text{Ph})$	73.6	0.13	0.27	1.00	31
	$[\kappa^2\text{-N}_3\text{O-PhC}(\text{O})\text{C}_6\text{H}_4\text{N}=\text{C}(\text{Ph})\text{OB}(\text{C}_6\text{F}_5)_3]\text{Ni}(\eta^3\text{-CH}_2\text{Ph})$	75.1	0.17	0.32	1.00	29
	$\{[\text{NH}(\text{Me})\text{CH}_2\text{CH}_2(\eta^3\text{-C}_5\text{H}_4)](\text{CO})\text{Re}(\eta^3\text{-CH}_2\text{Ph})\}^+\text{ReO}_4^-$	76.4	0.14	0.34	1.01	24
	$(\text{NHC-}2,6\text{-Pr}^i_2\text{-C}_6\text{H}_3)(\text{CF}_3\text{SO}_3)\text{Ni}(\eta^3\text{-CH}_2\text{Ph})$	76.4	0.20	0.41	1.13	27
	$[\text{Cp}^*\text{Zr}(\eta^3\text{-CH}_2\text{Ph})(\eta^7\text{-CH}_2\text{Ph})][\text{B}(\text{CH}_2\text{Ph})(\text{C}_6\text{F}_5)_3]$	87.7	0.36	0.41	1.44	1f
	$[(\text{Me}_3\text{Si})_2\text{NC}(\text{NCy})_2]_2\text{Er}(\eta^3\text{-CH}_2\text{Ph})$	90.6	0.38	0.51	1.39	22
	$[(\text{Me}_3\text{Si})_2\text{NC}(\text{NCy})_2]_2\text{Y}(\eta^3\text{-CH}_2\text{Ph})$	90.9	0.41	0.50	1.49	22
η^7	$[\text{Cp}^*\text{Zr}(\eta^3\text{-CH}_2\text{Ph})(\eta^7\text{-CH}_2\text{Ph})][\text{B}(\text{CH}_2\text{Ph})(\text{C}_6\text{F}_5)_3]$	62.1	−0.30	−0.12	−0.10	1f

^aNote that compounds with multiple benzyl ligands have an entry for each structurally different benzyl ligand.

Cambridge Structural Database (Figure 6) indicates that the only compound with both $\delta_{\text{ortho(short)}}$ and $\delta_{\text{ortho(long)}}$ < 0.5 Å is the η^7 -benzyl complex $[\text{Cp}^*\text{Zr}(\text{CH}_2\text{Ph})_2]^+$.^{1f} As such, despite the fact that η^4 -benzyl complexes are frequently considered,^{1,8a} there are no benzyl compounds listed in the Cambridge Structural Database that can be clearly assigned such a coordination mode according to the criteria listed in Table 4.³² In this regard, of the η^3 -complexes that are listed in the Cambridge Structural Database, the compound that most closely approaches η^4 -coordination is $\text{Me}_3\text{PNi}(\text{CH}_2\text{Ph})_2$, for which $\delta_{\text{ortho(short)}}$ = 0.33 Å and $\delta_{\text{ortho(long)}}$ = 0.76 Å.²⁸

According to the criteria listed in Table 4, two of the benzyl ligands in the monoclinic form of $\text{Zr}(\text{CH}_2\text{Ph})_4$ are coordinated in an η^1 -manner, while two are coordinated in an η^2 -manner (Table 2), as illustrated by their location in Figure 5. Specifically, the two η^2 -benzyl ligands have acute Zr–CH₂–

Ph angles of 81.6(1)° and 82.4(1)°, while the two η^1 -benzyl ligands have obtuse Zr–CH₂–Ph angles of 98.7(2)° and 106.7(2)°. In addition, the two η^2 -benzyl ligands have $\delta_{\text{ortho(short)}}$ values of 0.75 and 0.69 Å, which indicate that there is little η^3 -character associated with the interaction. Similar analysis for the orthorhombic form of $\text{Zr}(\text{CH}_2\text{Ph})_4$ classifies three of the benzyl ligands as η^2 [with Zr–CH₂–Ph angles of 87.0(3)°, 90.2(3)° and 93.9(3)°] and one as η^1 [with a Zr–CH₂–Ph angle of 99.1(3)°], as illustrated in Figure 5.

Examination of structurally characterized zirconium compounds indicates that the flexibility of benzyl ligands is by no means restricted to $\text{Zr}(\text{CH}_2\text{Ph})_4$, such that Zr–CH₂–Ph angles that range from 62.1°^{1f} to 144.4°¹⁶ in different compounds have been reported. The ability of crystal packing forces to influence zirconium–benzyl interactions has been reported by Arnold, who noted that $\{\text{CyNC}[\text{N}(\text{SiMe}_3)_2]\text{NCy}\}\text{Zr}(\text{CH}_2\text{Ph})_3$

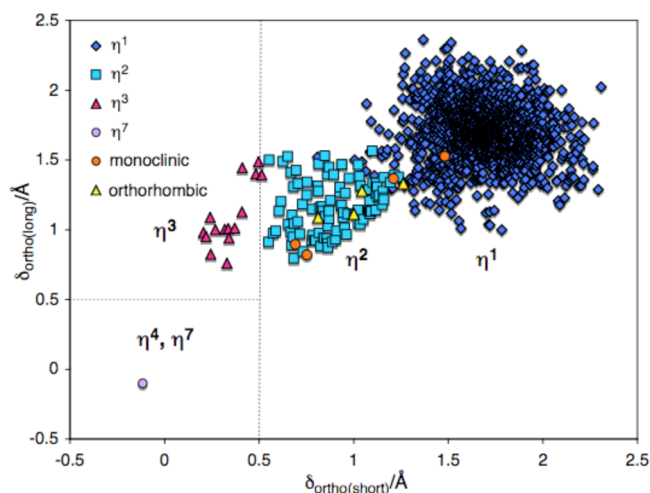


Figure 6. Classification of benzyl ligands according to $\delta_{\text{ortho(short)}}$ and $\delta_{\text{ortho(long)}}$.

exists as two polymorphs with Zr–CH₂–Ph angles that span the ranges 88.7(4)–123.2(4)° and 104.6(2)–115.9(2)°. ¹g.³³ Furthermore, a particularly interesting example of the flexibility of the benzyl ligand is provided by the observation that (Cp^{1,2,4}-Bu³)CeCH₂Ph exists with two distinctly different geometries in the asymmetric unit, with Ce–CH₂–Ph bond angles of 93.1(4)° and 130.4(3)°. ³⁴

Consistent with the inequivalent nature of the benzyl ligands in the solid-state structure of Zr(CH₂Ph)₄, the solid-state ¹³C{¹H} NMR spectrum exhibits a 1:1:2 set of signals for the four methylene carbon atoms at 76.4, 74.2 and 70.9 ppm, respectively (Figure 7), rather than a single resonance. In

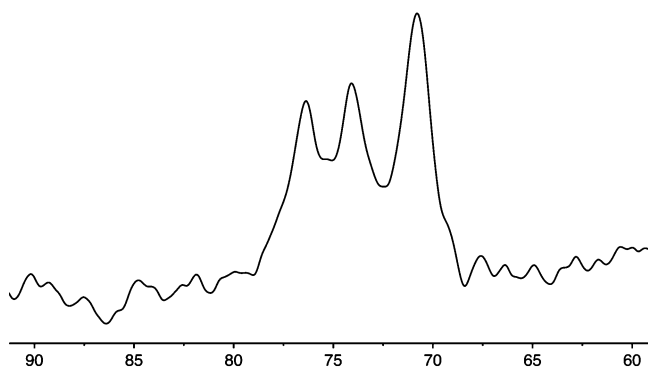


Figure 7. Solid-state ¹³C NMR spectrum of Zr(CH₂Ph)₄ (methylene region).

solution, however, the benzyl ligands are chemically equivalent on the NMR time-scale,³⁵ as illustrated in Figures 8 and 9. Spectroscopically, η^1 -coordination of benzyl ligands is associated with $\delta_{\text{H}_{\text{ortho}}} > 6.5$, $\delta_{\text{C}_{\text{ipso}}} \approx 150$, and $^1J_{\text{C-H}}$ for the CH₂ group of ~ 120 Hz, while η^2 -coordination is identified by $\delta_{\text{H}_{\text{ortho}}} < 6.5$, $\delta_{\text{C}_{\text{ipso}}} \approx 140$, and $^1J_{\text{C-H}}$ for the CH₂ group of ~ 135 Hz.³⁶ In this regard, Zr(CH₂Ph)₄ is characterized by $\delta_{\text{H}_{\text{ortho}}} = 6.38$, $\delta_{\text{C}_{\text{ipso}}} = 139.5$, and $^1J_{\text{C-H}} = 135$ for the CH₂ group, which support the presence of η^2 -benzyl ligands. However, while these values are in accord with the presence of some degree of η^2 -benzyl coordination in solution, they do not distinguish between a situation in which the η^2 -benzyl ligands are equivalent and one in which the molecule is

fluxional, and exchange between η^2 - and η^1 -benzyl ligands is facile.^{35a}

Computational Evaluation of the Flexibility of Benzyl Ligands Attached to Zirconium. In order to investigate the nature of Zr(CH₂Ph)₄ in solution, the molecular structure was investigated computationally by performing density functional theory (DFT) geometry optimization calculations (B3LYP). For this purpose, the geometry of Zr(CH₂Ph)₄ was optimized using (i) constrained Zr–CH₂–Ph bond angles that correspond to the monoclinic and orthorhombic structures, (ii) *S*₄ symmetry,³⁷ and (iii) no constraints. Significantly, the energies of each of these geometry-optimized structures (Figure 10) differ by < 2 kcal mol^{−1}, despite the fact that the Zr–C–C angles vary significantly between the structures (Table 6). This result is in accord with the observation that two different molecular structures of Zr(CH₂Ph)₄ could exist in the solid state.

To obtain a further appreciation of the energetic penalty associated with bending the Zr–C–C bonds, the *S*₄ symmetric structure was geometry optimized subject to constraining one of the Zr–C–C bond angles to a series of values that range from 70° to 150°. These data, as presented in Figure 11 and Table 7, indicate that one of the Zr–C–C bond angles can be varied over a large range without exerting a significant energetic penalty. For example, the energy of the molecule fluctuates by < 1.5 kcal mol^{−1} over the range 85–120°. However, constraining one of the Zr–C–C bond angles to a specific value is accompanied by changes in the other benzyl ligands to accommodate the induced perturbation, as illustrated by the variation in the range of Zr–C–C bond angles for each structure (Table 6). For this reason, the energy profile is not characterized by a single minimum.

In order to eliminate the buffering effect provided by the other benzyl ligands, geometry optimization calculations were also performed on Me₃ZrCH₂Ph, which features only one benzyl ligand. Significantly, while the most stable geometry-optimized structure possesses a Zr–C–C bond angle of 92.8°, the energy of the molecule changes by less than 2 kcal mol^{−1} over the range 80–125° (Figure 12). Thus, the flexibility of the benzyl ligands in Zr(CH₂Ph)₄ is not merely attributable to a buffering effect due to the presence of other benzyl ligands, but is intrinsic to the Zr–CH₂–Ph moiety. Specifically, the energy required to decrease the Zr–CH₂–Ph bond angle is compensated by interaction of the phenyl group with the electronically unsaturated zirconium center, while the energy required to increase the Zr–CH₂–Ph bond angle is compensated by the formation of agostic interactions with the methylene group,³⁸ as illustrated in Figure 13. For example, the large Ti–CH₂–Ph angle (139.0°) and short Ti...H interactions (2.32 and 2.37 Å) for one of the benzyl ligands of Cp^{*}Ti(CH₂Ph)₃ have been interpreted in terms of a double agostic interaction.³⁹ Furthermore, species with α -agostic interactions have also been proposed as intermediates in olefin polymerization catalyzed by [Cp₂Zr(CH₂Ph)]⁺.^{7k}

Comparison with the silicon counterpart, Me₃SiCH₂Ph, provides evidence that these secondary interactions with zirconium are responsible for the flexibility of the benzyl ligand of Me₃ZrCH₂Ph, because silicon does not form benzyl compounds with a very large range of Si–CH₂–Ph bond angles.^{40,41} Thus, not only is the Si–CH₂–Ph angle for the most stable structure (114.4°) much larger than that for the zirconium compound (92.8°), but the energy of the molecule increases substantially as the Si–CH₂–Ph angle deviates from

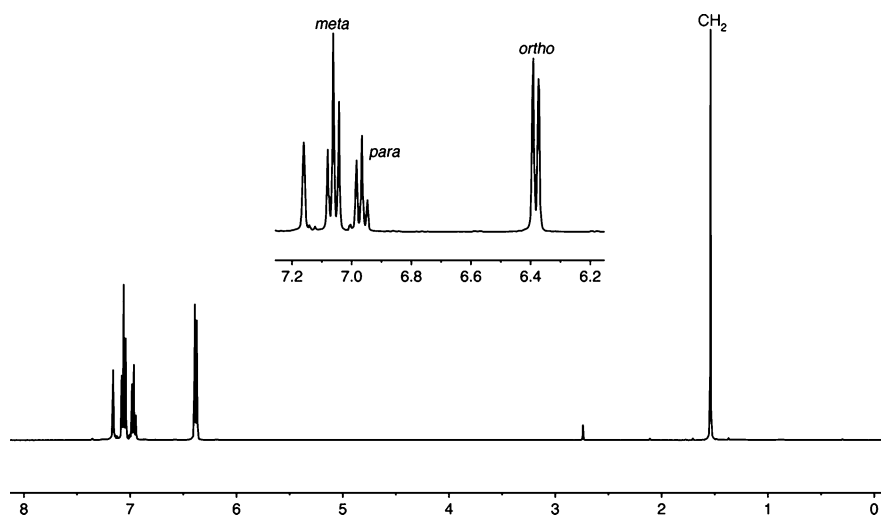


Figure 8. ^1H NMR spectrum of $\text{Zr}(\text{CH}_2\text{Ph})_4$.

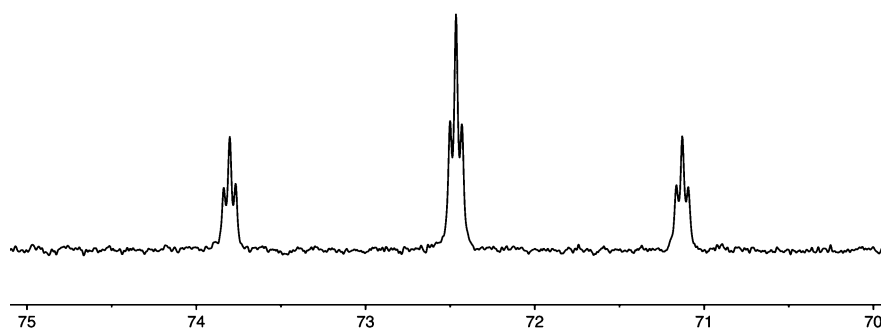


Figure 9. ^{13}C NMR spectrum of $\text{Zr}(\text{CH}_2\text{Ph})_4$ (methylene region).

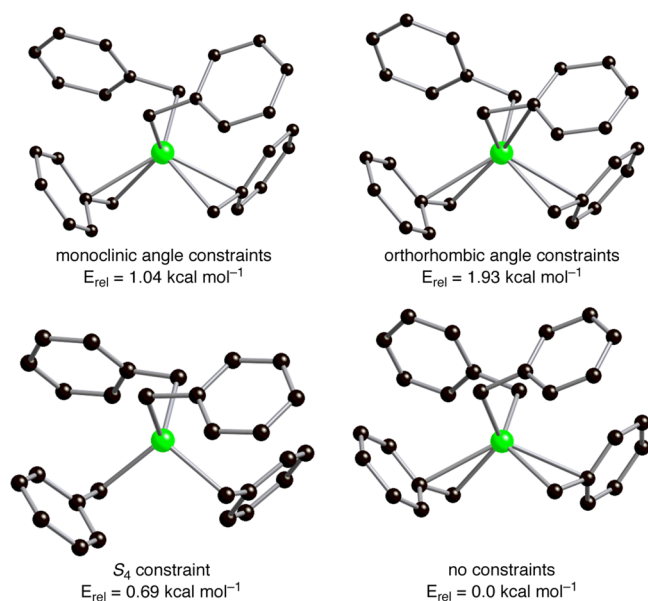


Figure 10. Geometry-optimized structures of $\text{Zr}(\text{CH}_2\text{Ph})_4$ subject to various constraints.

this value (Figure 12). For example, reducing the $\text{Si}-\text{CH}_2-\text{Ph}$ bond angle to 85° increases the energy of the molecule by $19.1 \text{ kcal mol}^{-1}$, while increasing the angle to 150° increases the energy to $14.3 \text{ kcal mol}^{-1}$, both of which are much greater than the corresponding values of 0.4 and $6.8 \text{ kcal mol}^{-1}$ for the zirconium system.

Table 6. Geometry-Optimized Structures for $\text{Zr}(\text{CH}_2\text{Ph})_4$

	$\text{Zr}-\text{C}-\text{C}/\text{deg}$				relative energy/ kcal mol^{-1}
no constraints	87.7	87.9	105.1	106.1	0.00
S_4 symmetry	100.2	100.2	100.2	100.2	0.69
monoclinic ^a	81.7	82.4	98.6	106.7	1.04
orthorhombic ^b	87.1	90.2	93.9	99.0	1.93

^aGeometry-optimized structure with $\text{Zr}-\text{CH}_2-\text{Ph}$ angles constrained to those of the monoclinic structure. ^bGeometry-optimized structure with $\text{Zr}-\text{CH}_2-\text{Ph}$ angles constrained to those of the orthorhombic structure.

CONCLUSIONS

In summary, the $\text{Zr}-\text{CH}_2-\text{Ph}$ bond angles in the monoclinic modification of $\text{Zr}(\text{CH}_2\text{Ph})_4$ span a much larger range (25.1°) than those reported for the orthorhombic form (12.1°). Density functional theory calculations demonstrate that little energy is required to perturb the $\text{Zr}-\text{CH}_2-\text{Ph}$ bond angles in this compound, thereby providing support for the existence of two different molecular structures in the solid state. Furthermore, density functional theory calculations also indicate that bending of the $\text{Zr}-\text{CH}_2-\text{Ph}$ moiety in the monobenzyl compound $\text{Me}_3\text{ZrCH}_2\text{Ph}$ is facile, thereby demonstrating that a benzyl ligand attached to zirconium is intrinsically flexible, such that its bending does not require a buffering effect involving another benzyl ligand. This flexibility of the benzyl ligand could provide a means to protect a metal center during a catalytic transformation.^{5,7k} Despite this

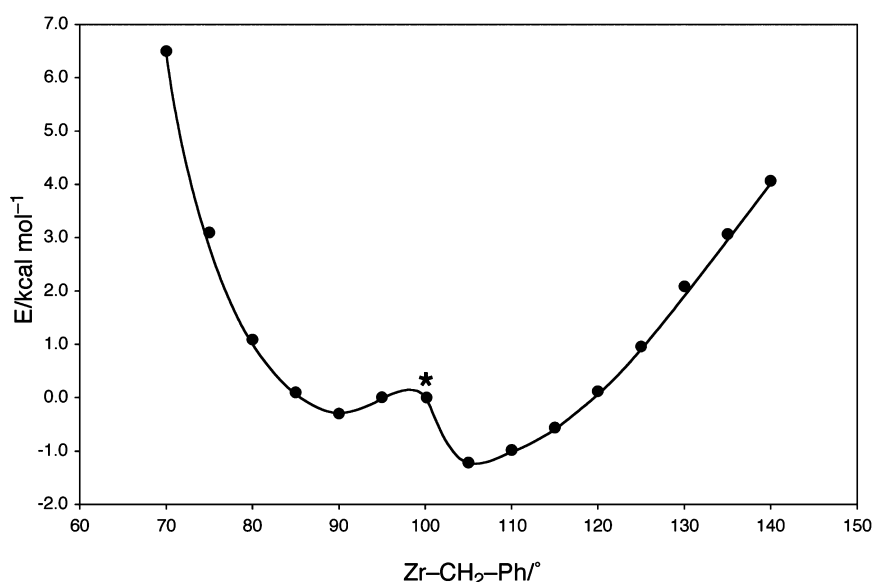


Figure 11. Variation in energy of $\text{Zr}(\text{CH}_2\text{Ph})_4$ as a function of varying a single $\text{Zr}-\text{CH}_2-\text{Ph}$ bond angle after allowing the geometry to reoptimize. The energies are relative to that of the S_4 constrained geometry, as indicated with an asterisk.

Table 7. Energy Changes Associated with Bending the $\text{Zr}-\text{C}-\text{C}$ Angle of One of the Benzyl Ligands (#1) in $\text{Zr}(\text{CH}_2\text{Ph})_4$

Zr-C-C/deg #1 constrained	Zr-C-C/deg #2	Zr-C-C/deg #3	Zr-C-C/deg #4	bond angle distribution/ deg	bond angle range/ deg	relative energy/ kcal mol ⁻¹
70.0	93.4	104.3	106.8	70.0–106.8	36.8	6.50
75.0	93.3	105.4	105.8	75.0–105.8	30.8	3.10
80.0	93.4	106.4	105.3	80.0–106.4	26.4	1.09
85.0	94.0	109.0	104.8	85.0–109.0	24.0	0.10
90.0	93.8	109.3	104.6	90.0–109.3	19.3	−0.30
95.0	93.9	110.3	104.5	93.9–110.3	16.4	−0.09
100.0	93.4	111.5	104.2	93.4–111.5	18.1	0.31
100.2 ^a	100.2 ^a	100.2 ^a	100.2 ^a	100.2	0.0	0.00
105.0	105.7	88.0	87.5	87.5–105.7	18.2	−1.22
110.0	105.7	87.4	88.2	87.4–110.0	22.6	−0.98
115.0	105.3	86.2	88.8	86.2–115.0	28.8	−0.56
120.0	105.1	86.1	89.6	86.1–120.0	33.9	0.12
125.0	105.7	89.3	91.1	89.3–125.0	35.7	0.96
130.0	105.4	91.8	94.5	91.8–130.0	38.2	2.09
135.0	98.9	101.7	88.8	88.8–135.0	46.2	3.07
140.0	102.7	95.9	88.0	88.0–140.0	52.0	4.07

^aGeometry-optimized value when constrained to S_4 symmetry.

flexibility, however, the majority of structurally characterized benzyl compounds feature η^1 -coordination modes.

EXPERIMENTAL SECTION

General Considerations. All manipulations were performed using a combination of glovebox, high-vacuum, and Schlenk techniques under an argon atmosphere unless otherwise specified.⁴² Solvents were purified and degassed by using standard procedures. ^1H NMR spectra were measured on Bruker 400 Cyber-enabled Avance III and Bruker 500 DMX spectrometers. ^1H chemical shifts are reported in ppm relative to SiMe_4 ($\delta = 0$) and were referenced internally with respect to the protio solvent impurity ($\delta = 7.16$ for $\text{C}_6\text{D}_5\text{H}$).⁴³ ^{13}C NMR spectra are reported in ppm relative to SiMe_4 ($\delta = 0$) and were referenced internally with respect to the solvent ($\delta = 128.06$ for C_6D_6).⁴³ Coupling constants are given in hertz. Solid-state $^{13}\text{C}\{^1\text{H}\}$ NMR experiments were performed on a Bruker 400 Cyber-enabled Avance III at a field of 9.40 T (corresponding to a ^{13}C resonance frequency of 100.62 MHz) using the CP-MAS pulse sequence, with an acquisition time of 0.03 s and a spin rate of 10^4 Hz. Solid-state ^{13}C NMR spectra

are reported in ppm relative to SiMe_4 ($\delta = 0$) and were referenced externally to the methylene peak of adamantane ($\delta = 38.5$).⁴⁴

Synthesis of $\text{Zr}(\text{CH}_2\text{Ph})_4$. $\text{Zr}(\text{CH}_2\text{Ph})_4$ was synthesized via the reaction of PhCH_2MgCl ⁴⁵ with ZrCl_4 by a modification of the literature method.^{3b} A solution of benzylchloride (13.6 g, 0.11 mol) in THF (200 mL) was slowly added to a stirred suspension of magnesium turnings (11.0 g, 0.45 mol) in THF (50 mL) over a period of ca. 1 h, such that the temperature of the reaction vessel was maintained at ca. 25 °C. The mixture was stirred at room temperature overnight and then filtered. The volatile components were removed from the filtrate *in vacuo* to give PhCH_2MgCl as an off-white powder, which was treated sequentially with ZrCl_4 (6.0 g, 0.026 mol) and Et_2O (150 mL) at −15 °C. The mixture was stirred at −15 °C overnight and filtered at 0 °C. The precipitate was washed with Et_2O (200 mL) at 0 °C and then extracted into toluene (200 and 100 mL). The volatile components were removed from each extraction *in vacuo*, resulting in the formation of $\text{Zr}(\text{CH}_2\text{Ph})_4$ as orange crystalline blocks suitable for X-ray diffraction (2.1 and 1.0 g, 26%). The synthesis and the purification of tetrabenzylzirconium were conducted in the absence of

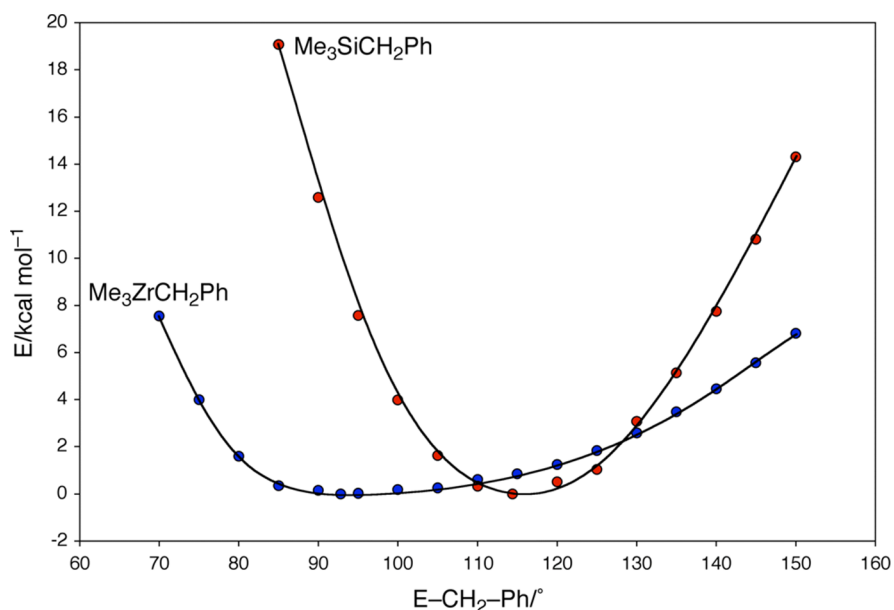


Figure 12. Variation in energy of $\text{Me}_3\text{ECH}_2\text{Ph}$ as a function of the $\text{E}-\text{CH}_2-\text{Ph}$ bond angle after allowing the geometry to reoptimize ($\text{E} = \text{Zr}, \text{Si}$).

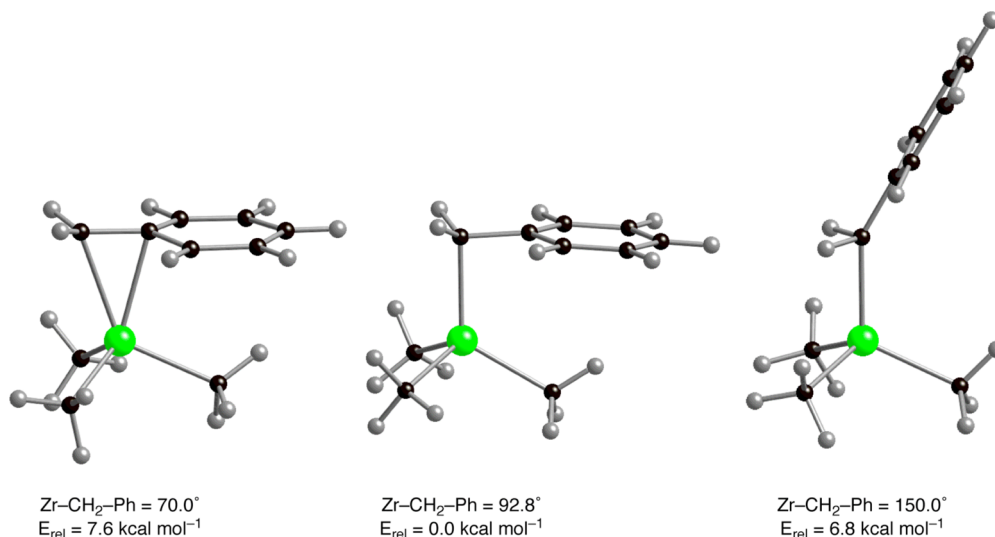


Figure 13. Geometry-optimized structures of $\text{Me}_3\text{ZrCH}_2\text{Ph}$. Reducing the $\text{Zr}-\text{CH}_2-\text{Ph}$ bond angle from that in the fully optimized structure (92.8°) is accompanied by an increased interaction with the phenyl group, while increasing the angle is accompanied by the formation of agostic interactions with the CH_2 group. The geometries have approximate C_s symmetry such that at acute angles the benzyl ligand approaches η^4 rather than η^3 coordination.

light to avoid any photochemical decomposition. ^1H NMR (C_6D_6): 1.55 [s, 8H of $\text{Zr}\{(\text{CH}_2)\text{C}_6\text{H}_5\}_4$], 6.38 [d, $^3J_{\text{H-H}} = 7$, 8H_{ortho} of $\text{Zr}\{(\text{CH}_2)\text{C}_6\text{H}_5\}_4$], 6.96 [t, $^3J_{\text{H-H}} = 7$, 4H_{para} of $\text{Zr}\{(\text{CH}_2)\text{C}_6\text{H}_5\}_4$], 7.06 [t, $^3J_{\text{H-H}} = 7$, 8H_{meta} of $\text{Zr}\{(\text{CH}_2)\text{C}_6\text{H}_5\}_4$]. ^{13}C NMR (C_6D_6): 72.5 [tt, $^1J_{\text{C-H}} = 135$, $^3J_{\text{C-H}} = 4$, 4C of $\text{Zr}\{(\text{CH}_2)\text{C}_6\text{H}_5\}_4$], 124.5 [dt, $^1J_{\text{C-H}} = 162$, $^3J_{\text{C-H}} = 8$, 4C_{para} of $\text{Zr}\{(\text{CH}_2)\text{C}_6\text{H}_5\}_4$], 128.7 [m, 8C_{ortho} of $\text{Zr}\{(\text{CH}_2)\text{C}_6\text{H}_5\}_4$], 131.0 [dd, $^1J_{\text{C-H}} = 159$, $^3J_{\text{C-H}} = 8$, 8C_{meta} of $\text{Zr}\{(\text{CH}_2)\text{C}_6\text{H}_5\}_4$], 139.5 [s, 4C_{ipso} of $\text{Zr}\{(\text{CH}_2)\text{C}_6\text{H}_5\}_4$]. Solid-state $^{13}\text{C}\{^1\text{H}\}$ NMR (only CH_2 group listed): 76.4 (1C), 74.0 (1C), 70.4 (2C) at -10°C ; 76.4 (1C), 74.2 (1C), 70.9 (2C) at room temperature; 76.4 (1C), 74.4 (1C), 71.1 (2C) at 50°C .

X-ray Structure Determinations. X-ray diffraction data were collected on a Bruker Apex II diffractometer. The structures were solved using direct methods and standard difference map techniques and were refined by full-matrix least-squares procedures on F^2 with SHELXTL (version 6.14).⁴⁶

Computational Details. Calculations were carried out using DFT as implemented in the Jaguar 7.6 (release 110) suite of *ab initio*

quantum chemistry programs.⁴⁷ Geometry optimizations were performed with the B3LYP density functional⁴⁸ using the 6-31G** (C, H, and Si) and LACVP (Zr) basis sets.⁴⁹

■ ASSOCIATED CONTENT

● Supporting Information

CIF files and Cartesian coordinates for geometry-optimized structures. This material is available free of charge via the Internet at <http://pubs.acs.org>.

■ AUTHOR INFORMATION

Corresponding Author

*E-mail: parkin@columbia.edu.

Notes

The authors declare no competing financial interest.

ACKNOWLEDGMENTS

We thank the U.S. Department of Energy, Office of Basic Energy Sciences (DE-FG02-93ER14339), for support of this research. A.A.-H. thanks the government of Saudi Arabia for a scholarship. Dr. John Decatur, Michael Appel, and Wenbo Li are thanked for assistance with the solid-state ^{13}C NMR experiments.

REFERENCES

- (1) (a) Edwards, P. G.; Andersen, R. A.; Zalkin, A. *Organometallics* **1984**, *3*, 293–298. (b) Legzdins, P.; Jones, R. H.; Phillips, E. C.; Yee, V. C.; Trotter, J.; Einstein, F. W. B. *Organometallics* **1991**, *10*, 986–1002. (c) Carmona, E.; Marin, J. M.; Paneque, M.; Poveda, M. L. *Organometallics* **1987**, *6*, 1757–1765. (d) Dryden, N. H.; Legzdins, P.; Trotter, J.; Yee, V. C. *Organometallics* **1991**, *10*, 2857–2870. (e) Scholz, J.; Rehbaum, F.; Thiele, K. H.; Goddard, R.; Betz, P.; Kruger, C. J. *Organomet. Chem.* **1993**, *443*, 93–99. (f) Pellicchia, C.; Immirzi, A.; Pappalardo, D.; Peluso, A. *Organometallics* **1994**, *13*, 3773–3775. (g) Giesbrecht, G. R.; Whitener, G. D.; Arnold, J. *Organometallics* **2000**, *19*, 2809–2812.
- (2) Although there are no η^5 -benzyl compounds listed in the Cambridge Structural Database, pentamethyl $\text{CH}_2\text{C}_6\text{Me}_5$ counterparts are known. See, for example: (a) Hamon, J. R.; Astruc, D.; Roman, E.; Batail, P.; Mayerle, J. J. *Am. Chem. Soc.* **1981**, *103*, 2431–2433. (b) Moler, J. L.; Eymann, D. P.; Nielson, J. M.; Morken, A. M.; Schauer, S. J.; Synder, D. B. *Organometallics* **1993**, *12*, 3304–3315.
- (3) (a) Zucchini, U.; Giannini, U.; Albizzati, E.; D'Angelo, R. J. *Chem. Soc. D, Chem. Commun.* **1969**, 1174–1175. (b) Zucchini, U.; Albizzati, E.; Giannini, U. *J. Organomet. Chem.* **1971**, *26*, 357–372.
- (4) Schrock, R. R.; Parshall, G. W. *Chem. Rev.* **1976**, *76*, 243–268.
- (5) Pedetour, J. N.; Radhakrishnan, K.; Cramail, H.; Deffieux, A. *Macromol. Rapid Commun.* **2001**, *22*, 1095–1123.
- (6) (a) Morton, C.; Munslow, I. J.; Sanders, C. J.; Alcock, N. W.; Scott, P. *Organometallics* **1999**, *18*, 4608–4613. (b) Gendler, S.; Segal, S.; Goldberg, I.; Goldschmidt, Z.; Kol, M. *Inorg. Chem.* **2006**, *45*, 4783–4790. (c) Tonzetich, Z. J.; Schrock, R. R.; Hock, A. S.; Muller, P. *Organometallics* **2005**, *24*, 3335–3342. (d) Turculet, L.; Tilley, T. D. *Organometallics* **2004**, *23*, 1542–1553. (e) Covert, K. J.; Mayol, A. R.; Wolczanski, P. T. *Inorg. Chim. Acta* **1997**, *263*, 263–278. (f) Scott, M. J.; Lippard, S. J. *Inorg. Chim. Acta* **1997**, *263*, 287–299. (g) Lubben, T. V.; Wolczanski, P. T.; Vanduyne, G. D. *Organometallics* **1984**, *3*, 977–983. (h) Felten, J. J.; Anderson, W. P. *J. Organomet. Chem.* **1972**, *36*, 87–92.
- (7) (a) Chen, C.; Lee, H.; Jordan, R. F. *Organometallics* **2010**, *29*, 5373–5381. (b) Martin, A.; Uhrhammer, R.; Gardner, T. G.; Jordan, R. F.; Rogers, R. D. *Organometallics* **1998**, *17*, 382–397. (c) Pellicchia, C.; Grassi, A.; Zambelli, A. *J. Mol. Catal.* **1993**, *82*, 57–65. (d) Pellicchia, C.; Grassi, A.; Immirzi, A. *J. Am. Chem. Soc.* **1993**, *115*, 1160–1162. (e) Ahn, H.; Nicholas, C. P.; Marks, T. J. *Organometallics* **2002**, *21*, 1788–1806. (f) Cohen, A.; Kopilov, J.; Goldberg, I.; Kol, M. *Organometallics* **2009**, *28*, 1391–1405. (g) Cuomo, C.; Milione, S.; Grassi, A. *Macromol. Rapid Commun.* **2006**, *27*, 611–618. (h) Gauvin, R. M.; Kress, J. J. *Mol. Catal. A: Chem.* **2002**, *182*, 411–417. (i) Duchateau, R.; Abbenhuis, H. C. L.; van Santen, R. A.; Meetsma, A.; Thiele, S. K. H.; van Tol, M. F. H. *Organometallics* **1998**, *17*, 5663–5673. (j) Chen, Y. X.; Fu, P. F.; Stern, C. L.; Marks, T. J. *Organometallics* **1997**, *16*, 5958–5963. (k) Bochmann, M.; Lancaster, S. J. *Organometallics* **1993**, *12*, 633–640.
- (8) (a) Tedesco, C.; Immirzi, A.; Proto, A. *Acta Crystallogr. Sect. B, Struct. Sci.* **1998**, *B54*, 431–437. (b) Davies, G. R.; Jarvis, J. A. J.; Kilbourn, B. T. *J. Chem. Soc., Chem. Commun.* **1971**, 1511–1512. (c) Davies, G. R.; Jarvis, J. A. J.; Kilbourn, B. T.; Pioli, A. J. P. *J. Chem. Soc. D, Chem. Commun.* **1971**, 677.
- (9) Cambridge Structural Database (Version 5.33). 3D Search and Research Using the Cambridge Structural Database. Allen, F. H.; Kennard, O. *Chem. Des. Autom. News* **1993**, *8* (1), 1, 31–37.
- (10) The selected planes are those that contain the axis that corresponds most closely to a molecular S_4 axis. The angles between other planes are 68° and 88° .
- (11) Sanz, M.; Mosquera, M. E. G.; Cuenca, T.; de Arellano, C. R.; Schormann, M.; Bochmann, M. *Polyhedron* **2007**, *26*, 5339–5348.
- (12) Beckerle, K.; Manivannan, R.; Spaniol, T. P.; Okuda, J. *Organometallics* **2006**, *25*, 3019–3026.
- (13) Furthermore, a benzyl compound with a bond angle of 98.6° was described as possessing partial η^2 -character. See: Groysman, S.; Goldberg, I.; Kol, M.; Genizi, E.; Goldschmidt, Z. *Organometallics* **2003**, *22*, 3013–3015.
- (14) Other large $\text{M}-\text{CH}_2-\text{Ph}$ bond angles that have been assigned to η^2 -coordination include 94.5° ,^a 95.3° ,^b 95.8° ,^c 96.1° ,^d 96.3° ,^e and 96.7° .^f (a) Reference 1d. (b) Natrajan, L. S.; Wilson, C.; Okuda, J.; Arnold, P. L. *Eur. J. Inorg. Chem.* **2004**, 3724–3732. (c) Cariou, R.; Gibson, V. C.; Tomov, A. K.; White, A. J. P. *J. Organomet. Chem.* **2009**, *694*, 703–716. (d) Tsukahara, T.; Swenson, D. C.; Jordan, R. F. *Organometallics* **1997**, *16*, 3303–3313. (e) Chan, M. C. W.; Kui, S. C. F.; Cole, J. M.; McIntyre, G. J.; Matsui, S.; Zhu, N. Y.; Tam, K. H. *Chem.—Eur. J.* **2006**, *12*, 2607–2619. (f) Irwin, L. J.; Reibenspies, J. H.; Miller, S. A. *Polyhedron* **2005**, *24*, 1314–1324.
- (15) Mean = 2.685 Å; range = 2.592–2.762 Å.
- (16) Lee, H.; Jordan, R. F. *J. Am. Chem. Soc.* **2005**, *127*, 9384–9385.
- (17) Ziniuk, Z.; Goldberg, I.; Kol, M. *Inorg. Chem. Commun.* **1999**, *2*, 549–551.
- (18) Wiecko, M.; Girnt, D.; Rastatter, M.; Panda, T. K.; Roesky, P. W. *Dalton Trans.* **2005**, 2147–2150.
- (19) Qian, B. X.; Scanlon, W. J.; Smith, M. R.; Motry, D. H. *Organometallics* **1999**, *18*, 1693–1698.
- (20) Jordan, R. F.; Lapointe, R. E.; Baenziger, N.; Hinch, G. D. *Organometallics* **1990**, *9*, 1539–1545.
- (21) Mintz, E. A.; Moloy, K. G.; Marks, T. J.; Day, V. W. *J. Am. Chem. Soc.* **1982**, *104*, 4692–4695.
- (22) Kiplinger, J. L.; Morris, D. E.; Scott, B. L.; Burns, C. J. *Organometallics* **2002**, *21*, 5978–5982.
- (23) Zhang, Z.; Zhang, L.; Li, Y.; Hong, L.; Chen, Z.; Zhou, X. *Inorg. Chem.* **2010**, *49*, 5715–5722.
- (24) Wang, T.-F.; Hwu, C.-C.; Tsai, C.-W.; Wen, Y.-S. *J. Chem. Soc., Dalton Trans.* **1998**, 2091–2096.
- (25) Bleeke, J. R.; Burch, R. R.; Coulman, C. L.; Schardt, B. C. *Inorg. Chem.* **1981**, *20*, 1316–1318.
- (26) Fryzuk, M. D.; McConville, D. H.; Rettig, S. J. *J. Organomet. Chem.* **1993**, *445*, 245–256.
- (27) Sujith, S.; Noh, E. K.; Lee, B. Y.; Han, J. W. *J. Organomet. Chem.* **2008**, *693*, 2171–2176.
- (28) Wasilke, J.-C.; Ziller, J. W.; Bazan, G. C. *Adv. Synth. Catal.* **2005**, *347*, 405–408.
- (29) Shim, C. B.; Kim, Y. H.; Lee, B. Y.; Shin, D. M.; Chung, Y. K. *J. Organomet. Chem.* **2003**, *675*, 72–76.
- (30) Chen, Y.; Boardman, B. M.; Wu, G.; Bazan, G. C. *J. Organomet. Chem.* **2007**, *692*, 4745–4749.
- (31) Zhou, X.; Bontemps, S.; Jordan, R. F. *Organometallics* **2008**, *27*, 4821–4824.
- (32) A reviewer has suggested that the paucity of benzyl complexes that feature η^4 -coordination could be a consequence of it being energetically unfavorable to disrupt a six-membered aromatic ring into two allyl components. In contrast, η^3 -coordination of the benzyl ligand disrupts the ring in such a manner as to leave an isolated butadiene moiety.
- (33) For a recent review of crystal packing effects on bond lengths, see: Minasian, S. G.; Krinsky, J. L.; Arnold, J. *Chem.—Eur. J.* **2011**, *17*, 12234–12245.
- (34) Werkema, E. L.; Andersen, R. A.; Maron, L.; Eisenstein, O. *Dalton Trans.* **2010**, 39, 6648–6660.
- (35) (a) Latesky, S. L.; McMullen, A. K.; Niccolai, G. P.; Rothwell, I. P.; Huffman, J. C. *Organometallics* **1985**, *4*, 902–908. (b) Scholz, J.; Schlegel, M.; Thiele, K. H. *Chem. Ber. Recl.* **1987**, *120*, 1369–1374.
- (36) Oulié, P.; Freund, C.; Saffon, N.; Martin-Vaca, B.; Maron, L.; Bourissou, D. *Organometallics* **2007**, *26*, 6793–6804.

(37) The geometry-optimized S_4 geometry is characterized by a τ_4 parameter of 0.8, where $\tau_4 = [360 - (\alpha + \beta)]/141$ and $\alpha + \beta$ is the sum of the two largest angles. For comparison, a tetrahedral geometry has a τ_4 parameter of 1.0. See: Yang, L.; Powell, D. R.; Houser, R. P. *Dalton Trans.* **2007**, 955–964.

(38) (a) Brookhart, M.; Green, M. L. H.; Parkin, G. *Proc. Natl. Acad. Sci. U. S. A.* **2007**, *104*, 6908–6914. (b) Brookhart, M.; Green, M. L. H.; Wong, L. L. *Prog. Inorg. Chem.* **1988**, *36*, 1–124. (c) Brookhart, M.; Green, M. L. H. *J. Organomet. Chem.* **1983**, *250*, 395–408.

(39) Mena, M.; Pellinghelli, M. A.; Royo, P.; Serrano, R.; Tiripicchio, A. *Chem. Commun.* **1986**, 1118–1119.

(40) The mean Si–CH₂–Ph bond angle for compounds listed in the Cambridge Structural Database is 115.0°, with a range of 106.3–120.8°.

(41) Calculations were performed on Me₃SiCH₂Ph rather than Me₃CCH₂Ph because silicon is capable of adopting coordination numbers greater than 4, which is required if the benzyl ligand is to adopt an expanded hapticity.

(42) (a) McNally, J. P.; Leong, V. S.; Cooper, N. J. In *Experimental Organometallic Chemistry*; Wayda, A. L.; Darensbourg, M. Y., Eds.; American Chemical Society: Washington, DC, 1987; Chapter 2, pp 6–23. (b) Burger, B. J.; Bercaw, J. E. In *Experimental Organometallic Chemistry*; Wayda, A. L.; Darensbourg, M. Y., Eds.; American Chemical Society: Washington, DC, 1987; Chapter 4, pp 79–98. (c) Shriver, D. F.; Drezdson, M. A. *The Manipulation of Air-Sensitive Compounds*, 2nd ed.; Wiley-Interscience: New York, 1986.

(43) Gottlieb, H. E.; Kotlyar, V.; Nudelman, A. *J. Org. Chem.* **1997**, *62*, 7512–7515.

(44) Morcombe, C. R.; Zilm, K. W. *J. Magn. Reson.* **2003**, *162*, 479–486.

(45) Benkeser, R. A.; Snyder, D. C. *J. Org. Chem.* **1982**, *47*, 1243–1249.

(46) (a) Sheldrick, G. M. *SHELXTL*, An Integrated System for Solving, Refining and Displaying Crystal Structures from Diffraction Data; University of Göttingen: Göttingen, Germany, 1981. (b) Sheldrick, G. M. *Acta Crystallogr.* **2008**, *A64*, 112–122.

(47) *Jaguar 7.6*, Schrödinger, LLC: New York, NY, 2009.

(48) (a) Becke, A. D. *J. Chem. Phys.* **1993**, *98*, 5648–5652. (b) Becke, A. D. *Phys. Rev. A* **1988**, *38*, 3098–3100. (c) Lee, C. T.; Yang, W.; Parr, R. G. *Phys. Rev. B* **1988**, *37*, 785–789. (d) Vosko, S. H.; Wilk, L.; Nusair, M. *Can. J. Phys.* **1980**, *58*, 1200–1211. (e) Slater, J. C. *Quantum Theory of Molecules and Solids, Vol. 4: The Self-Consistent Field for Molecules and Solids*; McGraw-Hill: New York, 1974.

(49) (a) Hay, P. J.; Wadt, W. R. *J. Chem. Phys.* **1985**, *82*, 270–283. (b) Wadt, W. R.; Hay, P. J. *J. Chem. Phys.* **1985**, *82*, 284–298. (c) Hay, P. J.; Wadt, W. R. *J. Chem. Phys.* **1985**, *82*, 299–310.